JOURNAL OF ENVIRONMENTAL SCIENCES 125 (2023) 603–615

Available online at www.sciencedirect.com

ScienceDirect

www.elsevier.com/locate/jes

JES JOURNAL OF ENVIRONMENTAL SCIENCES

www.jesc.ac.cn

Evidence of aircraft activity impact on local air quality: A study in the context of uncommon airport operation

Hao Xu[1,7], *Kai Xiao*[2], *Jun Pan*[3], *Qingyan Fu*[3], *Xiaodong Wei*[4,5], *Junrui Zhou*[2], *Yamei Yu*[3], *Xue Hu*[1,6], *Huarui Ren*[1], *Jinping Cheng*[1,*], *Shitao Peng*[7], *Ningning Hong*[7], *Yin Ye*[7], *Ning Su*[7], *Zehui He*[7], *Tao Hu*[7]

[1] *School of Environmental Science and Engineering, Shanghai Jiao Tong University, Shanghai 200240, China*
[2] *Wuhan Environmental Protection Science Academy, Wuhan 430015, China*
[3] *Shanghai Environmental Monitoring Center, Shanghai 200233, China*
[4] *Jiangsu Key Laboratory of Atmospheric Environment Monitoring and Pollution Control, Collaborative Innovation Center of Atmospheric Environment and Equipment Technology, School of Environmental Science and Engineering, Nanjing University of Information Science & Technology, Nanjing 210044, China*
[5] *East China Air Traffic Management Bureau CAAC, Shanghai 200335, China*
[6] *China-UK Low Carbon College, Shanghai 201306, China*
[7] *Tianjin Research Institute for Water Transport Engineering, Ministry of Transport, Tianjin 300456, China*

ARTICLE INFO

Article history:
Received 26 May 2021
Revised 15 October 2021
Accepted 22 February 2022
Available online 7 March 2022

Keywords:
Aircraft emissions
COVID-19
Nitrogen oxides
Ozone
Airport closure

ABSTRACT

Wuhan Tianhe International Airport (WUH) was suspended to contain the spread of COVID-19, while Shanghai Hongqiao International Airport (SHA) saw a tremendous flight reduction. Closure of a major international airport is extremely rare and thus represents a unique opportunity to straightforwardly observe the impact of airport emissions on local air quality. In this study, a series of statistical tools were applied to analyze the variations in air pollutant levels in the vicinity of WUH and SHA. The results of bivariate polar plots show that airport SHA and WUH are a major source of nitrogen oxides. NO_x, NO_2 and NO diminished by 55.8%, 44.1%, 76.9%, and 40.4%, 33.3% and 59.4% during the COVID-19 lockdown compared to those in the same period of 2018 and 2019, under a reduction in aircraft activities by 58.6% and 61.4%. The concentration of NO_2, SO_2 and $PM_{2.5}$ decreased by 77.3%, 8.2%, 29.5%, right after the closure of airport WUH on 23 January 2020. The average concentrations of NO, NO_2 and NO_x scatter plots at downwind of SHA after the lockdown were 78.0%, 47.9%, 57.4% and 62.3%, 34.8%, 41.8% lower than those during the same period in 2018 and 2019. However, a significant increase in O_3 levels by 50.0% and 25.9% at WUH and SHA was observed, respectively. These results evidently show decreased nitrogen oxides concentrations in the airport vicinity due to reduced aircraft activities, while amplified O_3 pollution due to a lower titration by NO under strong reduction in NO_x emissions.

* Corresponding author.
E-mail: jpcheng@sjtu.edu.cn (J.P. Cheng).

https://doi.org/10.1016/j.jes.2022.02.039
1001-0742/

Introduction

Aviation is an integral part of the global transportation system and contributes significantly to the world's economy (Lee et al., 2009; ICAO, 2019); however, while aviation enables economic prosperity, it represents one of the most intensive energy consumers and its emissions impose adverse impacts on the climate, surface air quality and human health (Morris et al., 2003; Lee et al., 2010; Carslaw et al., 2006). Aircraft emissions impose direct radiative effects on the climate system through emissions of carbon dioxide (CO_2), soot, and water vapor (H_2O) (Olsen et al, 2013), while nitrogen oxides (NO_x), sulfur oxides (SO_x), carbon monoxide (CO), and hydrocarbons (HC) emitted from aircraft operations have indirect radiative impacts through their interactions with complex gaseous and aerosol processes affecting ozone, methane, and clouds (Holmes et al., 2011), occurring at roughly 9 - 11 km (Morris et al., 2003; Lee et al., 2010). Pollutants emitted during landing and take-off cycle (LTO) can lead to air quality deterioration (Carslaw et al., 2006; Barrett et al., 2010; Lee et al., 2013). Previous studies have shown that aircraft emissions can substantially deteriorate surface air quality by increasing the concentrations of NO_x (Carslaw et al., 2006), CO (Schürmann et al., 2007), $PM_{2.5}$ (Unal et al., 2005; Hu et al., 2009) and the level of hazardous airborne particle-bound polycyclic aromatic hydrocarbons (PB-PAH), vapor-phase PAH (Childers et al., 2000) and particle-bound lead (PBL) concentrations (Fine, 2007) in the vicinity of airports. Ozone (O_3) is a secondary pollutant, which is generated through a series of photochemical reactions between its precursors, nitrogen oxides ($NO_x = NO + NO_2$) and volatile organic compounds (VOCs) (Liu et al., 2012). The formation of O_3 is much depending on the O_3 sensitivity regime, determined by the ratio of VOCs and NO_x (Lu et al., 2010). Studies also reported that aircraft activities contribute positively to elevated O_3 level (Yim et al., 2015; Ashok et al., 2013). Additionally, aircraft emissions are recognized to cause premature mortality (Barrett et al., 2010; Levy et al., 2012; Yim et al., 2015), and deleterious consequences for human health, e.g., increased incidence of cardiovascular and pulmonary diseases, asthma, diabetes and cancers, have been linked to elevated NO_x and PM concentrations (Hertel et al., 2013; Shiraiwa et al., 2017).

A few studies have attempted to estimate the negative contribution of aircraft activities to local air quality. These studies were generally implemented through site measurements or modelling work. For example, Hudda et al. (2014) measured the particle number concentrations (PNC) and a 2-5-fold increase in areas 8-16 km downwind of the Los Angeles International Airport (LAX) was observed, while Hu et al. (2009) reported elevated ultrafine particles (UFPs) concentrations by a factor of 10 and 2.5 at 100 and 660 m downwind, respectively, and spikes in concentration of black carbon (BC) and particle-bound polycyclic aromatic hydrocarbons (PB-PAH) were in association with aircraft activities. The nitrogen oxides detected in individual plumes from aircraft departing on the northern runway of London Heathrow Airport (LHR) demonstrate that concentrations of NO_x can be affected by operational factors such as take-off weight and aircraft thrust setting (Masiol and Harrison, 2015). In the case of aircraft emission modeling, Song et al. (2015) investigated the impact of aircraft emissions on O_3 concentrations in the vicinity of three international airports with Weather Research and Forecasting (WRF) and the Community Multiscale Air Quality (CMAQ), and a noticeable impact on the concentrations of O_3 and NO_x was detected. CMAQ modeling results by Unal et al. (2005) indicate that the maximum impact of aircraft activities at Hartsfield–Jackson Atlanta International Airport (ATL) can be as high as 56 ppb hourly, while a national-scale estimate shows that LTO emissions contributed 0.05% (3.2 ng/m^3) to the total $PM_{2.5}$ in the U.S. in 2005 and this would be 0.20% (11.2 ng/m^3) in 2025 (Woody et al., 2011). Additionally, statistical models were also used to quantify the aircraft and airport related emissions on local air quality on the basis of measured air pollutant concentrations. For instance, Carslaw et al. (2006) identified that airport operations of LHR contributed approximately 27% of the annual mean NO_x at the downwind airfield boundary. However, all these studies were implemented under "normal running" of airports, none have initiated a straightforward observation of aircraft activity impact under specific conditions, e.g. a complete airport closure.

In December 2019, an outbreak of atypical pneumonia occurred in Wuhan, Hubei province, China, which was later identified to be caused by a novel coronavirus, named after severe acute respiratory syndrome coronavirus 2 (SARS-CoV-2). The World Health Organization (WHO) characterized the coronavirus disease 2019 (COVID-19) as a "pandemic" (WHO, 2020). Till today, the ongoing global pandemic remains the most significant health concern. To contain the spread of COVID-19, China adopted unprecedented nationwide interventions, including the quarantine of the whole Wuhan city (Xinhua Net, 2020). All the road and railway traffic to and from Wuhan were suspended, the airport in Wuhan was also closed since 10 o'clock of January 23 2020. Meanwhile, Shanghai launched the first-level response to major public health emergencies on 25 January. Due to the strict controls on travel and large-scale quarantine, an abundance of flights to and from Shanghai Hongqiao International Airport (SHA) were cancelled.

The closure of Wuhan Tianhe International Airport (WUH) resulted in flight-ban at WUH (only an extremely small amount of cargo and medical personnel flights) and suspension of related airport activities (e.g., ground service equipment (GSE), auxiliary power unit (APU)). SHA also saw a significant reduction in aircraft activities. Decline in emissions from aircraft activities and other airport related sources thus could reasonably be expected at airport WUH and SHA. The closure of a major international airport and a tremendous drop in flights for a duration of over two months are extremely rare, and as such represent a unique opportunity to investigate the effect of airport emissions on the near-field air quality.

This study initiates a novel perspective on the impact of COVID-19 related lockdown, from the perspective of reduced aircraft activities on air quality. We applied a series of statistical tools to analyze the air pollutant concentrations measured at airport WUH and SHA before and during the airport closure (WUH) and significant flight reduction (SHA). Both measuring sites are located in the close vicinity of the airports. The main objectives of this study are: i) investigating the potential sources of air pollutants; ii) identifying the difference between

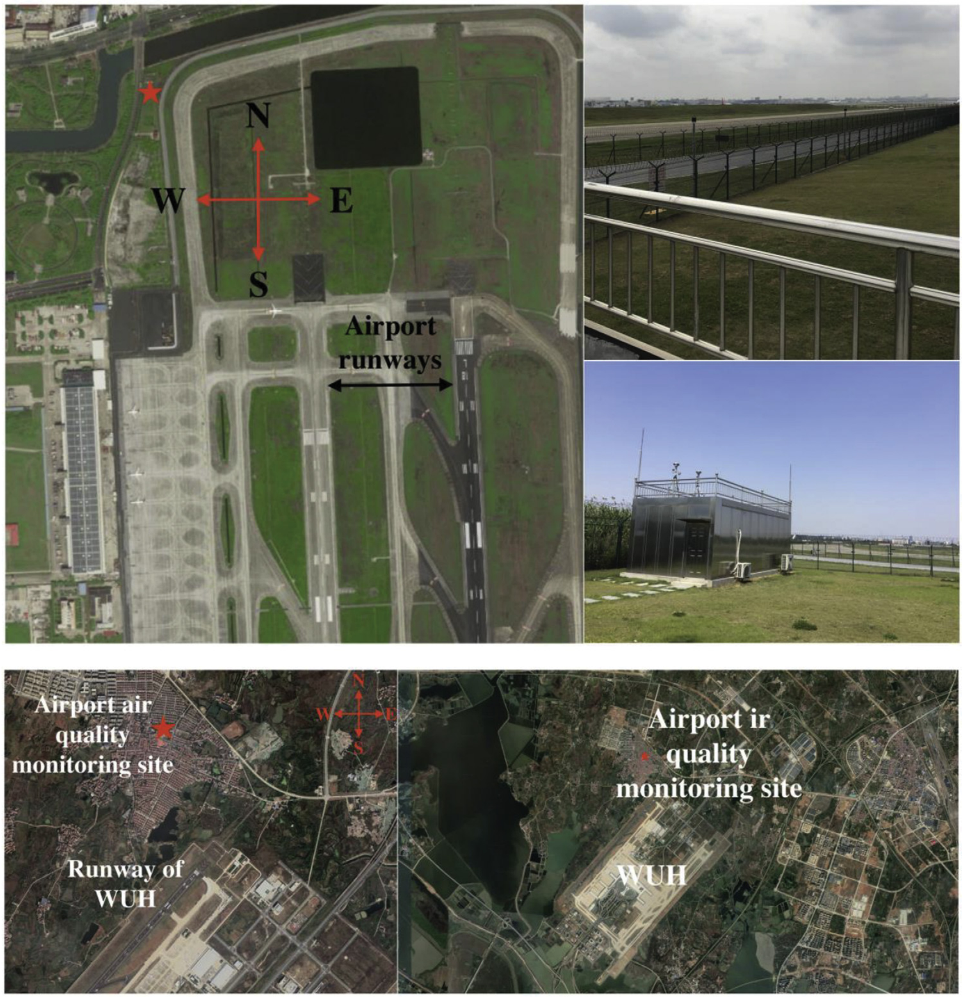

Fig. 1 – Map of the study areas depicting the measuring stations at SHA (upper) and WUH (lower).

long-term trends of air pollutant levels and those during the COVID-19 outbreak; iii) revealing the dependence of air pollutant concentrations on aircraft movements, to recognize the impact of aircraft activity on the air quality in the vicinity of airport.

1. Methodology and material

1.1. Location and study data

The airport WUH is situated in the north of Wuhan, approximately 25 km from the city center. In 2019, WUH represents the 13th largest airport in China in terms of aircraft activity, increasing by 8.2% compared to that of 2018, while the SHA is the 10^{th} largest in aircraft movement (CAAC, 2020).

Air pollutants including NO_2, SO_2, CO, O_3, $PM_{2.5}$ and PM_{10} were measured at the monitoring station of WUH managed by Wuhan Ecological and Environmental Bureau. The measuring site at WUH is approximately 950 m north of the runway that situated in the west of the airport complex. A map of the measuring station is depicted in Fig. 1. While the measuring site of SHA is located on the boundary of the airfield and approximately 400 m from the runway. The locations of the SHA and the measuring station of SHA are detailed in Xu et al. (2020b). At the measuring site of SHA, NO_x, NO, NO_2, SO_2, CO, O_3, $PM_{2.5}$ and PM_{10} were measured using automatic instruments according to regulations issued by the Ministry of Environment and Ecology (MEE, 2018a, b). Quality assurance (QA) and quality control (QC) procedures follow the principles of the National Ambient Air Quality Urban Monitoring Network Management. BC is additionally measured at SHA using an AE-31 aethalometer by Magee Scientific Company. Taking into account the health effect of aircraft and other airport related emissions, the BTEX (1,3-butadiene, benzene, toluene, ethylbenzene, styrene, o-xylene, m, p-xylene) levels are also monitored via the AMA GC 5000 BTX online gas chromatograph, which was developed for continuous monitoring of organic pollutant (in the range of C4-C12) levels in ambient air on the basis of EU guideline 2002/3/EC, the VDI guideline 2100 and the guidelines of the Technical Assistance Document EPA/600-R-98/161 of the American Environmental Protection Agency (AMA, 2010). The AMA GC 5000 BTX analyzer has been configured, calibrated and the system has been specifically equipped according to the measurement requirements of SHA. The measuring stations at SHA and WUH are affected to

Table 1 – Characteristics of measuring stations: name and acronym, location, analyzed pollutants and periods of data availability.

Site	Acronym	Location (longitude, latitude)	Analyzed species	Date period
Shanghai Hongqiao International Airport	SHA	31.218, 121.328	$PM_{2.5}$, PM_{10}, NO, NO_2, NO_x, CO, SO_2, O_3	hourly data for 01/01/2016 – 10/03/2020
Shanghai Hongqiao International Airport	SHA	31.218, 121.328	BC, 1,3-butadiene, benzene, toluene, Ethylbenzene, styrene, o-xylene, m,p-xylene	hourly data for 01/01/2018 – 10/03/2020
Wuhan Tianhe International Airport	WUH	30.807, 114.216	$PM_{2.5}$, PM_{10}, NO_2, CO, SO_2, O_3	daily averages for 10/09/2019 – 03/03/2020, 5-minute data for 22/01/2020 – 23/01/2020

different degrees by the airport activities, as previous studies depicted that airport operations have an impact range of a few kilometers on NO_x concentrations (Carslaw et al., 2006) and ultrafine PNCs (Hudda et al., 2018).

Weather variables including wind direction, wind speed, atmospheric pressure, air temperature and relative humidity (RH) for SHA and WUH were provided by the Meteorological Center of East China Air Traffic Management Bureau and derived from the China Meteorological Data Service Center, respectively.

Another key dataset used in this study is the information on aircraft take-offs and landings at SHA and WUH. These data were provided by the Feiyou Technology Co., Ltd., which include the date and time of departure/arrival, whether the aircraft was arriving or departing, the type of aircraft e.g. Boeing 747, the destination and origin. The detailed data from Feiyou Technology Co., Ltd. were carefully matched with the monthly statistic released by Civil Aviation Administration of China (CAAC). The data we obtained representing approximately 98% of the aircraft movements, while the remaining 2% are uncommon smaller aircrafts, thus in terms of emissions such as NO_x, the impact of these uncommon smaller aircrafts could be extremely slight and neglected given that the engine of the unrecorded aircrafts emitting much lower amount of pollutants. The aircraft activity data of SHA and WUH are summarized in Figure S1 to Figure S4.

1.2. *Statistical method*

The monitoring station names, acronyms, geographic coordinates, the measured pollutants and the periods of available data are summarized in Table 1. Preliminary data processing and cleaning were implemented to check the outliers and abnormal records of the dataset. The R version 3.6.2 (R Core Team, 2019) and a series of packages, including "Openair" (Carslaw and Ropkins, 2012; Carslaw, 2019) were applied to analyze the measured data of SHA and WUH.

2. Results and discussion

2.1. *Polar plot analysis*

Polar plots depict the joint variation of the concentration of a pollutant with wind speed and wind direction, which have been proved as a significant analyzing instrument in identifying and characterizing the potential sources of air pollution (Carslaw et al., 2006; Carslaw and Ropkins, 2012; Grange et al., 2016). Polar coordinates essentially map the pollutant concentrations with wind speed and direction as a continuous surface that are highly useful in providing directional information concerning the source type and characteristics as well as the wind speed dependence of concentrations (Carslaw et al., 2006; Jones et al., 2010), e.g., dispersion characteristics, street canyons (Tomlin et al., 2009; Carslaw and Ropkins, 2012) and airport emission sources (Carslaw et al., 2006; Masiol and Harrison, 2015) Carslaw et al. (2006). identified aircraft plumes on the basis of wind speed dependence upon NO_x concentrations.

Figures 2 and 3 show the polar plots of monitored species at SHA and WUH, respectively. Concentration and meteorological records of SHA were filtered, and only data for hours of a day mostly affected by airport activities, i.e. between 7:00 and 22:00, were used for the polar plot analysis. From Fig. 2, a few interesting features of measured species can be perceived. Firstly, high NO concentrations occurred under very low wind speeds from almost all wind directions, but there is an evident increment in NO concentrations as the wind came from southeast (corresponding to the direction of airport), northeast and northwest. NO_x concentrations are also found to be highest under low wind speed, but particularly in wind direction of southeast, northeast and northwest, while the highest NO_2 concentrations were recorded in wind direction of southeast, northeast and northwest under wind speeds of smaller than 5 m/s. This could be totally expected because the airport is located to the southeast of the measuring station and only 400 m away. And there is also an apparent indication of sources to the northeast and northwest. As the wind speed enhanced from any direction, the concentrations of NO_2, NO and NO_x show a decrease, and the lowest concentrations are observed under the highest wind speed in the wind direction of east. Secondly, the concentrations of $PM_{2.5}$, PM_{10}, SO_2 and CO were also highest under low wind speeds of less than 5 m/s, but dominantly in the direction of northwest. It is worth noting that in the direction of southeast, high concentrations of SO_2 in a range of wind speeds and high CO concentrations under high wind speeds (10-15 m/sec) are also depicted by the polar plot coordinates. On the contrary, the lowest concentrations of O_3 were under very low wind speed, which is different from other pollutants, while the highest concentrations of

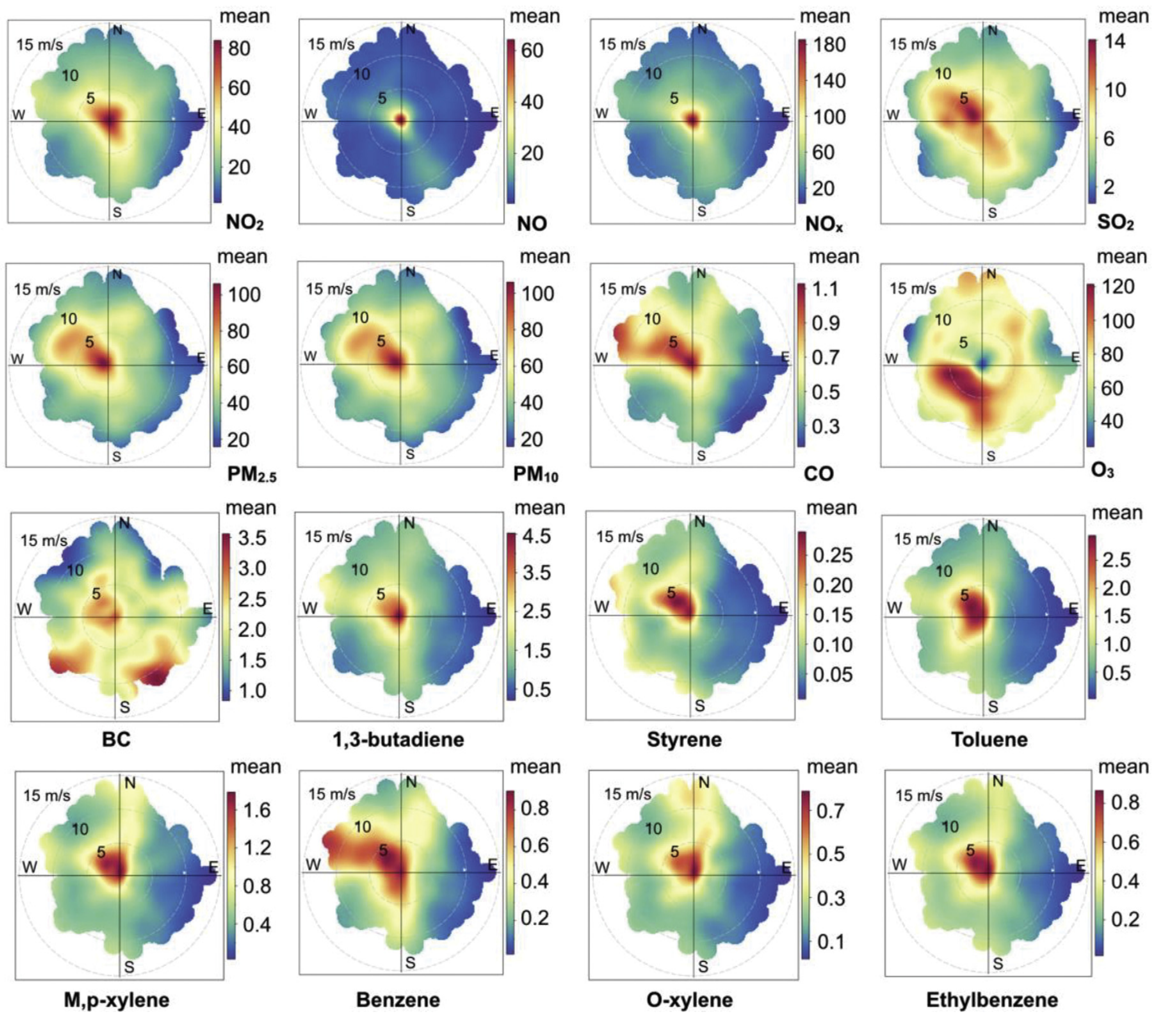

Fig. 2 – Bivariate polar plots for measured air pollutants at SHA.

O_3 were in the direction of south to west under wind speeds around 5 m/s. For BC, high concentrations were observed in the wind direction of northwest, however the highest concentrations were observed under high wind speeds (higher than 10 m/sec) in the direction of SHA. In the case of BTEX concentrations, the polar plot coordinates suggest a possible major source in northwest, as the concentrations of all BTEX species were highest under wind speeds below 5 m/s, and dominantly in the direction of northwest. The lowest BTEX concentrations were presented under high wind speeds in the wind direction of east.

With regard to the variations of air pollutant concentrations by wind direction and wind speed at WUH, it is interesting to note that the NO_2 concentrations were highest under very stable atmosphere (wind speed within 1 m/s), and were particularly observed in the southeast, corresponding to direction of airport WUH, as presented in Fig. 3. The highest concentrations of $PM_{2.5}$ and PM_{10} appeared under the wind speed range of 1-3 m/s in the wind direction of northeast and southeast, while there is an apparent increasing in SO_2, CO and O_3 concentrations when wind speeds were around 2 m/s, particularly in the southeast. The concentrations of measured pollutants at WUH decreased with increased wind speed and the lowest concentrations appeared in the north.

On the basis of the polar plot analysis above, it can be concluded that both SHA and WUH can be identified as a major contributor of nitrogen oxides. This could be entirely expected, as many previous studies have revealed that aircraft operations lead to increase in local nitrogen oxides concentrations (Carslaw et al., 2012; Masiol and Harrison, 2015). However, the O_3 concentrations show no distinct directionality in its source locations. The reason can be that O_3 is a secondary photochemical air pollutant. The formation of O_3 is subjected to solar radiation and its precursors, i.e., NO_x and VOCs (Sillman, 1995). The chemical mechanism of O_3 production and the relationship between O_3 and its precursors are complicated (Wang et al., 2017) and an important feature of O_3 production is that the dependence of O_3 production on its precursors is highly nonlinear (Zhang et al., 2008). O_3 concentrations could also be affected by the dispersion and transport effect, consequently, the O_3 concentrations may be related to other sources of precursors in long distance. The formation

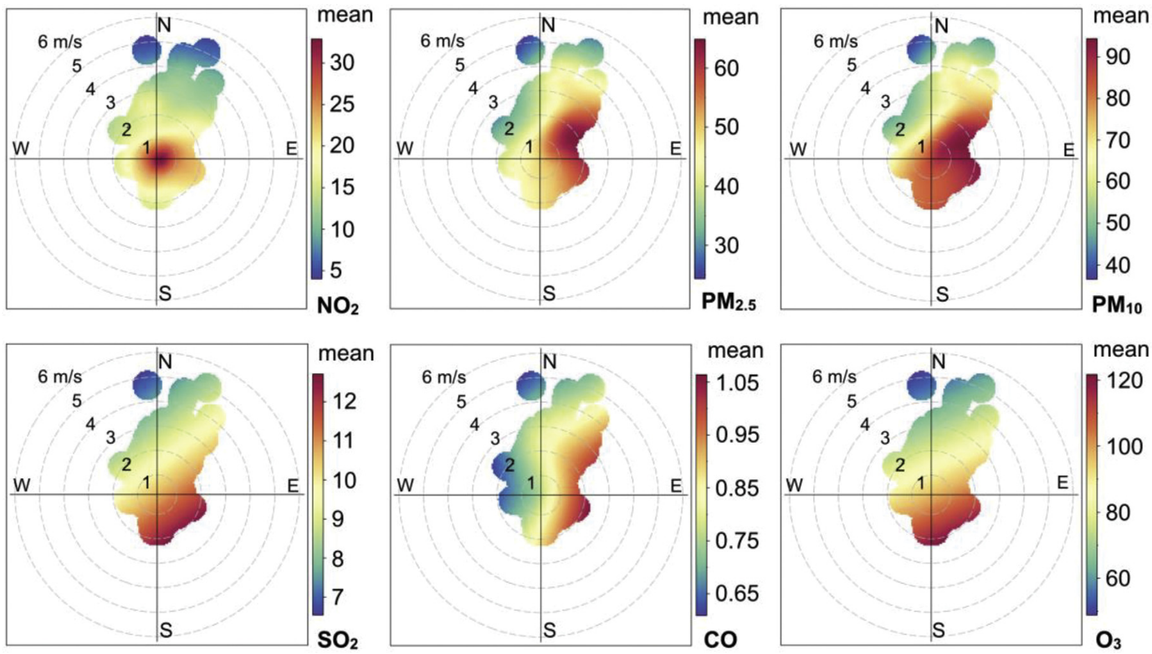

Fig. 3 – Polar plots for measured air pollutants at WUH.

of O_3 in the vicinity of airport and the association between O_3 production and airport operations deserves further investigation.

2.2. *Long-term trends analysis*

The concentrations of air pollutants measured at SHA in long-term trends were analyzed. A plot of monthly concentrations with smooth line fitted and the 95% confidence intervals of the fit were generated. The smooth line is essentially established on the basis of Generalized Additive Modelling with "mgcv" package (Carslaw, 2019). An indication of the overall trend on a monthly basis was determined by deseasonalizing the data using the "stl" function. The results are summarized in Fig. 4. The smooth lines in Fig. 4 represent the long-term trends of air pollutants concentrations at SHA, while the bands along with the smooth lines indicate the 95% confidence intervals of the fits.

In general, seasonal and weekly fluctuations of $PM_{2.5}$, SO_2, CO, O_3 and BTEX concentrations can be observed (detailed in Figure S5 and Figure S6), but an apparent decrease in PM_{10}, NO_x, NO_2 and SO_2 concentrations in 2020 was shown by the smooth lines, while the concentrations of O_3 saw a slight increasing trend. BC shows an even dramatic drop in 2020. To contain the spread of COVID-19, Shanghai launched the first-level response mechanism for major public health emergencies on 25 January 2020, and the impact of COVID-19 related lockdown on airport activity became evident in February. The number of landed and departed flights at SHA diminished significantly by 65.6% and 67.7% compared to the same month in 2018 and 2019 as shown Figure S1, respectively, resulting in a considerable reduction in NO_x, NO_2, NO, $PM_{2.5}$ and PM_{10} levels by 51.7%, 38.3%, 73.7%, 20.2% and 33.4% compared to those in 2018, and 45.1%, 17.4%, 22.4% and 22.1% in 2019, respectively. During the COVID-19 lockdown (25 January 2020 to 10 March 2020) period, the aircraft movements saw a dramatic reduction by 58.6% and 61.4% compared to those in the same period of 2018 and 2019, correspondingly, a notable decrease in the concentration of monitored species was observed, e.g., BTEX decreased by 34.8% to 68.7% and 31.6% to 61.9%, compared with those in the same period of 2018 and 2019, respectively. The main sources of BTEX species are fuel combustion in vehicle engines, fossil fuel burning, petroleum refining and storage, surface coatings, and use of solvents (Alyuz and Alp 2014; Dumanoglu et al. 2014; Hien et al. 2014). However, studies have shown that in the urban environment, fuel combustion represents the most important source. It has been reported that no more than 5-10% of the BTEX emissions in ambient air originate from non-automobile sources, and thus BTEX can be used as a proxy for traffic intensity (Bolden et al., 2015). Several studies have also demonstrated that airports are a "hotspot" for BTEX due to a variety of fuel-related activities (Amini et al., 2017; Jung et al., 2011). Thus, the reduced BTEX concentrations are reasonably correlated to declined aircraft activities. Additionally, the B/T ration (benzene to toluene) during the same period of lockdown in 2018 and 2019 were 0.44 and 0.55, which are comparable with those of other airports with 0.40 and 0.57 (Jung et al., 2011; Yang et al., 2018). However, during the lockdown period in 2020, the B/T ration is 0.93, which may suggest that the air quality is affected by the long-range transport of pollutants that has been photochemically degraded by the OH radical rather than by fresh local emissions that are rich in toluene (Beyer et al., 2003).

NO_x, NO_2 and NO diminished by 55.8%, 44.1% and 76.9% when comparing with those in the same period of 2018, and 40.4%, 33.3% and 59.4% in the same period of 2019. As concluded in the polar plot analysis, airport activities can be a major contributor of NO_x concentrations at SHA, the reduction

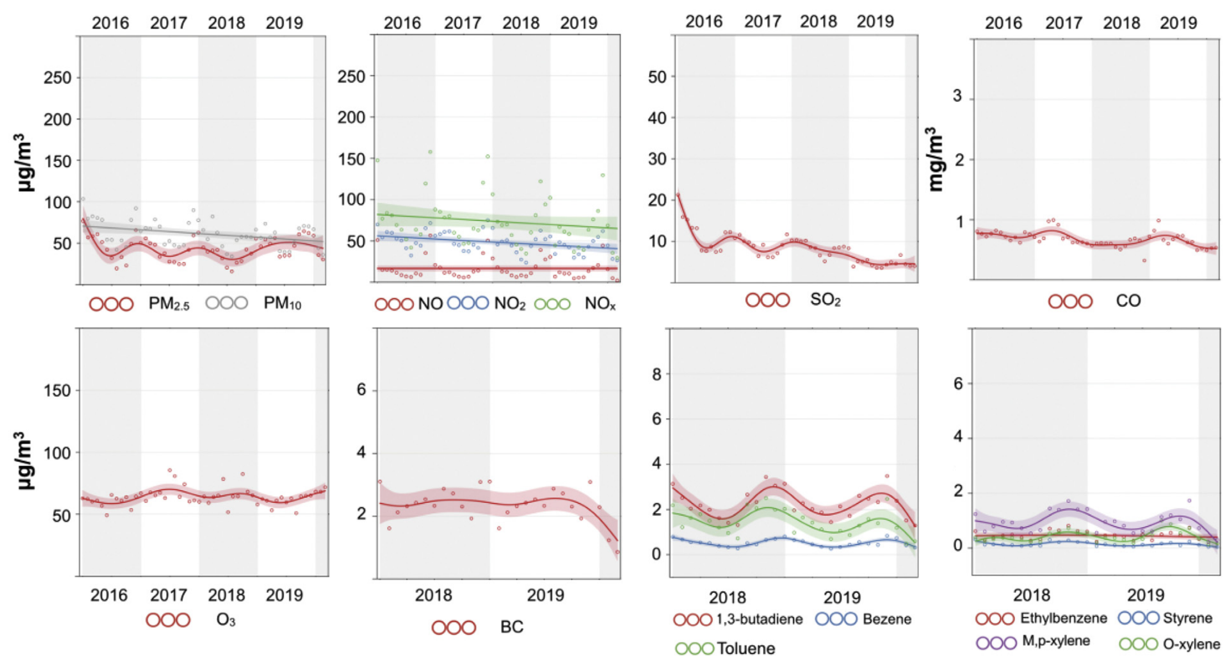

Fig. 4 – Long-term trends of air pollutants concentration levels at SHA.

in nitrogen oxides concentrations was highly correlated to the decrease of aircraft movements and related airport operations. A Pearson analysis also shows strong statistical associations between the decreased level of nitrogen oxides concentrations and decline in aircraft movements, as shown in Table S1. Decreased concentration of NO_x and NO_2 under flight-ban at London Heathrow Airport during the eruption of Eyjafjallajökull was also observed (Carslaw et al., 2012). A general decrease is also observed in the concentrations of other pollutants, such as $PM_{2.5}$, PM_{10}, BC, CO and SO_2. However, on the contrary, a perceptible increase in the O_3 concentrations during the COVID-19 lockdown was observed, which leveled off by 15.6% and 18.4%. The mean O_3 concentration in February 2020 was 6.6% and 10.1% higher than that in February of 2018 and 2019, respectively.

A long-term trend analysis of air pollutant concentrations at WUH was not performed, because the measuring site at WUH was not in operation until September 2019, and the smooth trend is commonly used to determine the trends over several years (Carslaw, 2019). Instead, the basic line plot function was applied. Figure S7 and 5 show the time series for all the measured air pollutants and the comparison of pollutant concentrations and aircraft movements during the same hours before (22 January 2020) and right after the suspension of WUH (23 January 2020). From Figure S7, an evident reduction in NO_2 concentrations since the closure of WUH can be observed, while the O_3 level was low in winter times, but shows an increasing trend since the closure of WUH. The aircraft movements in January and February 2020 at WUH reduced by 17.3% and 95.1% compared with that in December 2019, and only 85.3% and 5.0% of the monthly mean number of flights over the last 24 months (2018 and 2019), as depicted in Figure S3. As a result, the NO_2 concentrations saw a dramatic decrease by 61.2% and 87.9%, and considerable reduction in SO_2, $PM_{2.5}$ and PM_{10} concentrations were also perceived. In contrast, the level of O_3 increased by 9.2% and 46.4%. Figure 5 depicts the comparison between aircraft activity and the concentration of measured air pollutants on a 5-minute basis before and right after the closure of airport WUH. Aircraft activity saw a dramatic fall by 84.3% and dropped to 0 at 23 o'clock on 23 January 2020. The air pollutant concentrations on 22 January 2020 were evidently higher than those on 23 January 2020, NO_2, SO_2, CO, $PM_{2.5}$ and PM_{10} decreased by 77.3%, 8.2%, 10.8%, 29.5% and 23.9%, respectively, while O_3 concentration was higher on 23 January 2020 till around 15:00 than that on 22 January 2020, but lower afterwards. The unprecedented closure of airport WUH has an evident impact on the concentration of air pollutants and this effect has dropped the NO_2 concentration even to near zero. As also has been observed at Gatwick Airport and Heathrow Airport that local NO_2 has fallen to zero or near zero during the eruption of Eyjafjallajökull in April 2010 (Barratt and Fuller, 2010).

An increase in O_3 concentrations at both SHA and WUH was observed during the COVID-19 lockdown. Studies concerning the formation of O_3 show that the local O_3 formation is VOCs-limited in Wuhan (Zeng et al., 2018) and Shanghai (Xing et al., 2017; Ran et al., 2009; Cai et al., 2010; Tan et al., 2019), and a VOCs to NO_x ratio of no higher than 0.73 could be conducive to the O_3 pollution mitigation in Wuhan (Zeng et al., 2018). Song et al. (2015) demonstrates that area in the vicinity of airports VOC-limited. However, emission estimates for various airports have shown that aircraft operations during LTO emit significantly more NO_x than HCs (Unal et al., 2005; Kesgin, 2006; Stettler et al., 2011; Xu et al., 2020a), which can also be observed from the reduction rate of NO_x and BTEX concentrations during the COVID-19 lockdown as depicted above. During the closure of WUH and travel restriction at SHA, more NO_x emissions than VOCs emissions were reduced, resulting

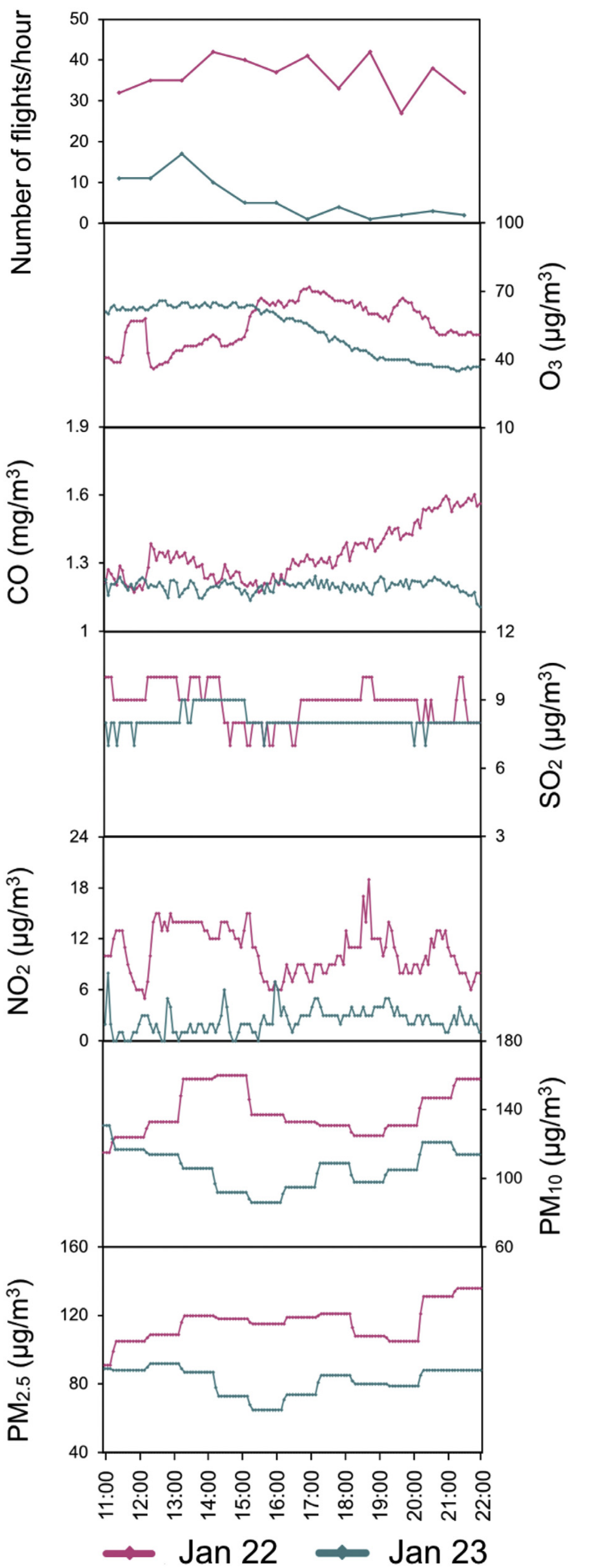

Fig. 5 – Comparison of pollutant concentrations and aircraft activity during the same hours before (22 Jan 2020) and right after the closure of airport WUH (23 Jan 2020).

in higher VOCs-NO_x ratio, which then strengthens the O_3 generation. The fresh exhausted NO emissions consume O_3 locally (Solberg et al., 2005; Molina et al., 2009). Aircraft and APU nitrogen oxides are predominantly emitted in the form of NO (Stettler et al., 2011) and the O_3 titration occurs particularly in winter times under high NO_x levels (Sillman, 1999), thus a lower titration of O_3 by NO due to strong reduction in local NO_x emissions (Sicard et al., 2020) may promote the increase in local O_3 concentrations during airport closure. Additionally, higher solar radiation due to lower $PM_{2.5}$ and PM_{10} concentrations (Murphy et al., 2007; Wolff et al., 2013) in the vicinity of WUH and SHA during the COVID-19 lockdown may also favor the O_3 formation. Furthermore, the long-range transport of O_3 precursors, such as VOC species, that has been photochemically degraded by the OH radical, may cause changes in VOCs emissions and thus impact the O_3 formation.

2.3. *Scatter plots analysis*

Scatter plots are extremely effective analyzing technique and can be used for examining the correlations between variables (Carslaw, 2019). The scatter plot analysis provides a straightforward demonstration of how two variables are related to one another on the dependence of a third variable. Here we applied the scatter plot function in "openair" to investigate the temporal variation of air pollutant concentrations before and during the COVID-19 lockdown depending on aircraft movements at SHA and WUH. Figure 6 depicts the hourly concentration of NO, NO_2 and NO_x under various aircraft movements at SHA for the period of 1 January to 31 March of 2018 and 2019, and 1 January to 10 March 2020, respectively. Dates and concentration levels were handled on the x-axis and y-axis, respectively, while the number of hourly flights was coded as a color scale shown to the right. The concentration data of NO, NO_2 and NO_x at SHA were filtered and only the data during the hours of intensive aircraft activity and downwind of the airport were considered in the scatter plot depiction. As such, a straightforward demonstration of the aircraft activity impact on the concentration of air pollutants can be seen.

As shown in Fig. 6, a significant distinction between the distribution of scatter plots for 2018 and 2019, and that for 2020 is observed. The scatter plots demonstrated for 2020 can be evidently divided into two groups, one of the groups are colored in blue, green and light yellow, indicating lower aircraft movements, and obviously on the days during the COVID-19 lockdown policy on the right side of the figures, while plots before the lockdown policy are in red and darkred, and positioned in upper zone of the figures, suggesting higher level of aircraft activity and concentrations. In contrast, a clear division in the distribution of the scatter plots for 2018 and 2019 cannot be observed. The average concentrations of NO, NO_2 and NO_x scatter plots during lockdown were 78.0%, 47.9%, 57.4% and 62.3%, 34.8%, 41.8% lower than those during the same period for 2018 and 2019, respectively. Studies have shown that aircraft and APU nitrogen oxides are predominantly emitted in the form of NO (Stettler et al., 2011; Xu et al., 2020a). This explains the largest drop in NO concentrations. BTEX and other air pollutants also saw a significant reduction in concentration levels as shown in Figure S8, e.g., $PM_{2.5}$ diminished by 21.5% and 48.4%

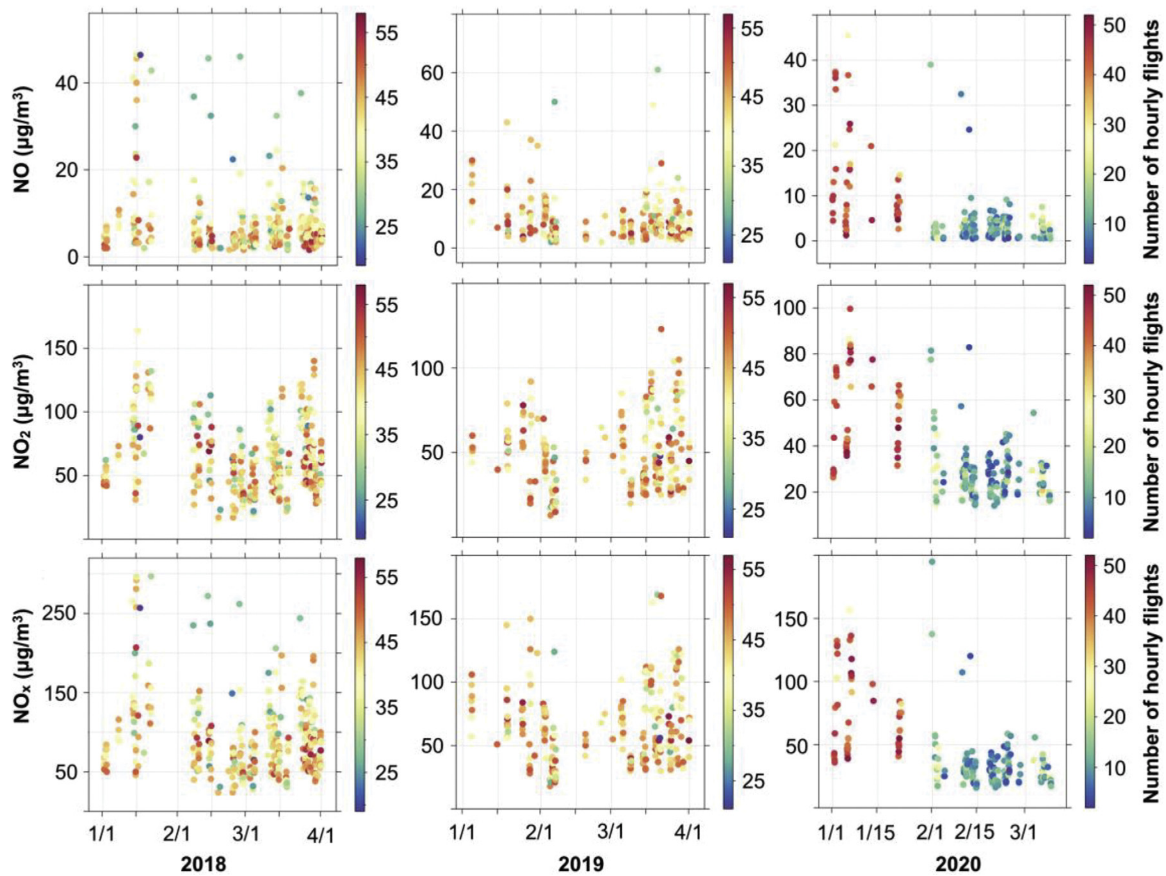

Fig. 6 – Scatter plot of date vs. nitrogen oxides at SHA by different levels of aircraft activity before and after the COVID-19 lockdown in 2020 and those during the same period of 2018 and 2019.

compared with those for 2018 and 2019, respectively. However, O_3 level increased by 11.1% and 25.9%, when the average hourly number of flights decreased by 66.4% and 66.8%. This may suggest that decreased aircraft activities contribute to elevated level of O_3 concentrations due to reduction in NO_x emissions.

From Fig. 7, the dependence of NO_2, $PM_{2.5}$, PM_{10}, SO_2, CO and O_3 concentrations upon the aircraft operations at WUH before and during the airport closure is depicted. Daily concentration averages of air pollutants and aircraft movements were used for generating the scatter plots for WUH. The distribution of scatter plots for NO_2 and O_3 of WUH is similar to that of SHA. A clear division of the scatter plots is observed. When comparing the concentration averages of the SO_2, NO_2, $PM_{2.5}$, PM_{10}, CO and O_3 scatter plots before (1 January 2020 to 22 January 2020) and during the closure of WUH (23 January 2020 to 3 March 2020), the average concentration of NO_2, $PM_{2.5}$, PM_{10}, CO during the airport closure were 79.3%, 28.4%, 32.4% and 21.5% lower than those before the closure of WUH, while a significant increase in O_3 concentrations by 50.0% under an unprecedented fall of aircraft movements by 95.2% during the closure of WUH was observed. Table S2 shows the correlations between individual air pollutant and aircraft activity. NO_2, $PM_{2.5}$, PM_{10} and CO concentrations were positively correlated with aircraft activity, while O_3 concentrations show a negative correlation. A strong correlation between NO_2 concentrations and aircraft activity can be found.

Restrictive measures in confining the COVID-19 pandemic contributed significant decline in greenhouse gas (GHG) and air pollutant emissions. Early estimates suggest that global GHG will decrease by 6% in 2020 compared to that in 2019, representing the largest fall since World War II (Stoll and Mehling, 2020), while air pollutant, such as NO_2, saw a steep fractional reduction by 93% at the peak of the COVID-19 outbreak in Wuhan (Le et al., 2020). The decline in aircraft activity at SHA and WUH is a microcosm of the decline in the global civil aviation that a lot of regions experienced a huge decline of more than 90% (IEA, 2020). Correspondingly, aviation emissions saw a significant decrease, e.g., GHG emissions declined by 74% during the early lockdown period (Stoll and Mehling, 2020) and reduction in air pollutant levels (NO_x, $PM_{2.5}$, etc.) as demonstrated in this study. Aviation plays a problematic role for climate change, air quality and human health (Chen and Sun, 2018; Lee et al., 2021), but the industry didn't react at the proper level on reducing emissions (Vaughan, 2020), and the probability of achieving all the environmental targets for aviation industry is extremely low (Hassan et al., 2018). Against this background, the COVID-19 pandemic may represent an opportunity to critically reconsider global aviation development and sustainability. Results in this study could be an implication of cleaner airport

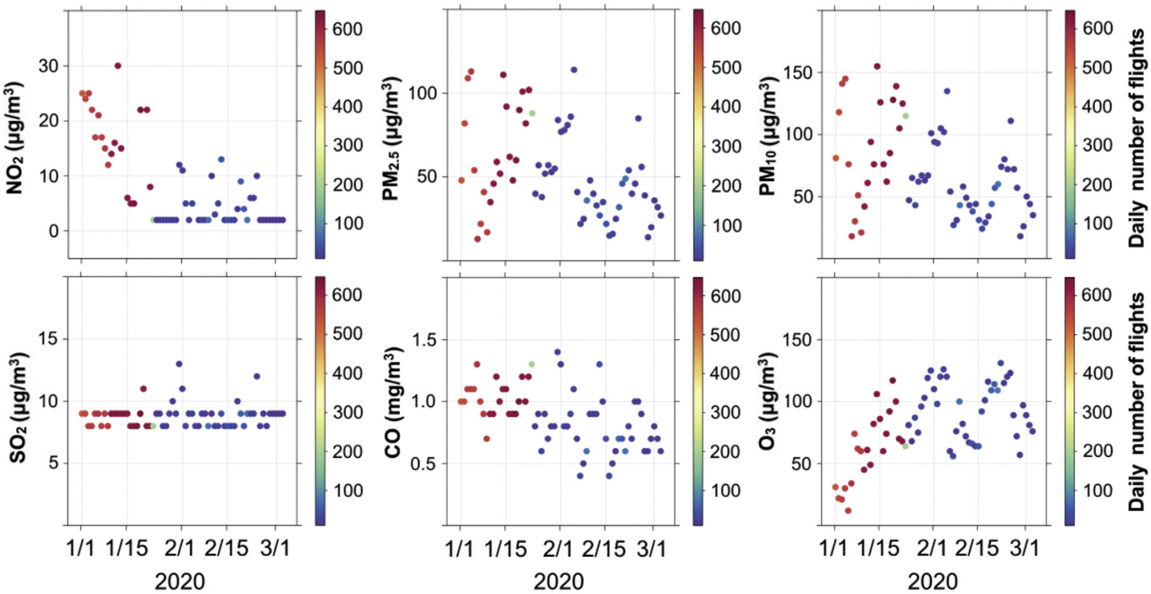

Fig. 7 – Scatter plot of date vs. measured air pollutant concentrations at WUH by different levels of aircraft activity before and after the COVID-19 lockdown in 2020.

operation. However, on the other hand, reduction in air pollutant emissions may not ensure direct improvement of air quality. The emissions-meteorology interactions (Mao et al., 2019), highly nonlinear ozone chemistry (Levy et al., 2014) may contribute significantly to air pollution even under marked emission reductions. The promoting effect of high humidity on aerosol heterogeneous chemistry, stagnant airflow and decrease in planetary boundary layer (PBL) height, facilitate positively the formation of secondary aerosol, while decrease in NO emissions removes the ozone titration leading to increase in ozone under reduction of NO_x (Levy et al., 2014); increased ozone further enhances the atmospheric oxidation capacity and facilitating again the secondary aerosol generation (Le et al., 2020). Therefore, as observed in this study, decreased aircraft activities contributed to reduced nitrogen oxides concentrations, but amplified O_3 pollution in the airport vicinity. Other studies have also revealed unexpected air pollution under remarkable emission reductions during COVID-19 lockdown period in China and other regions (Le et al., 2020; Wang et al., 2020; Adams, 2020). The key mechanism between aviation emissions and air quality deserves further investigation.

3. Conclusions

This study provides some indications of the impact of a specific emission source - airport activities, upon local air quality, from an unprecedented intervention by the COVID-19 epidemic, which has resulted in closure of airport WUH and significant reduction in aircraft activities at airport SHA. The closure of a major international is extremely rare, thus this study initiates a novel perspective on the impact of COVID-19 related lockdown on the air quality, from the perspective of reduced aircraft activities. The main results can be summarized as follows:

The polar plot analysis has highlighted the variations in the concentration of measured air pollutants with wind speed and wind direction at SHA and WUH. Aircraft and airport related emissions can be identified as major impact factor of nitrogen oxides. From the long-term trend analysis, an evident distinction between the concentration level on the long-term basis and those during the COVID-19 outbreak is observed, and a general decrease in the concentration of all pollutants (except O_3) is depicted. NO_x, NO_2 and NO at SHA diminished by 55.8%, 44.1% and 76.9% when comparing with those in the same period of 2018, and 40.4%, 33.3% and 59.4% of 2019. While at WUH, the NO_2 concentrations saw a dramatic decrease by 61.2% and 87.9% in January and February compared with that of December 2019, when the aircraft movements reduced by 17.3% and 95.1%, respectively. The concentration levels of NO_2, SO_2, CO, $PM_{2.5}$ and PM_{10} decreased by 77.3%, 8.2%, 10.8%, 29.5% and 23.9%, respectively, right after the closure of WUH on 23 Jan 2020, when compared with those at the same hours on 22 Jan 2020. Additionally, the distribution of scatter plots for both SHA and WUH depicts an evident distinction before and after the COVID-19 lockdown. It is shown that the concentration averages of NO, NO_2 and NO_x scatter plots after lockdown policy were 78.0%, 47.9%, 57.4% and 62.3%, 34.8%, 41.8% lower than those during the same period for 2018 and 2019 at SHA, respectively. At WUH, the average concentration of NO_2, $PM_{2.5}$, PM_{10}, CO after the airport closure were 79.3%, 28.4%, 32.4% and 21.5% lower than those before, and a Pearson analysis shows that NO_2, $PM_{2.5}$, PM_{10} and CO concentrations were significantly positively correlated with aircraft activity. However, O_3 level increased by 11.1% and 25.9% when the average hourly number of flights decreased by 66.4% and 66.8% at airport SHA, respectively, while a significant increase in O_3 concentrations by 50.0% under an unprecedented fall of aircraft movements by 95.2% after the closure of airport WUH was observed. These results depict that reduction in aircraft activities contributes to mitigation of NO_x pollution in the airport vicinity, but enhanced level of O_3 concentrations, which may be attributed to lower titration of O_3 by NO under strong reduction in NO_x emissions.

Acknowledgements

This work was supported by the Shanghai Municipal Bureau of Ecology and Environment (Environmental Research Project [2017]17 and [2018]10) and the Institute of Urban Governance, Shanghai Jiao Tong University (Key Special Project of China) No. SJTU-2019UGBD-01). We appreciate greatly the funding support. Any opinions, findings, and conclusions or recommendations expressed in this paper are those of the authors do not necessarily reflect the views of the sponsors.

Appendix A Supplementary data

Supplementary material associated with this article can be found, in the online version, at doi:10.1016/j.jes.2022.02.039.

REFERENCE

Adams, M.D., 2020. Air pollution in Ontario, Canada during the COVID-19 state of emergency. Sci. Total. Environ. 742, 140516. doi:10.1016/j.scitotenv.2020.140516.

Alyuz, U., Alp, K., 2014. Emission inventory of primary air pollutants in 2010 from industrial processes in Turkey. Sci. Total. Environ. 488–489, 369–381. doi:10.1016/j.scitotenv.2014.01.123.

AMA Instruments GmbH, 2010. Operating Manual Gas chromatograph – GC 5000 BTX. Ulm, Germany.

Amini, H., Hosseini, V., Schindler, C., Hassankhany, H., Yunesian, M., Henderson, S.B., et al., 2017. Spatiotemporal description of BTEX volatile organic compounds in a Middle Eastern megacity: Tehran study of exposure prediction for environmental health research (Tehran SEPEHR). Environ. Pollut. 226, 219–229. doi:10.1016/j.envpol.2017.04.027.

Ashok, A., Lee, I.H., Arunachalam, S., Waitz, I.A., Yim, S.H.L., Barrett, S.R.H., 2013. Development of a response surface model of aviation's air quality impacts in the United States. Atmos. Environ. 77, 445–452. doi:10.1016/j.atmosenv.2013.05.023.

Zeng, P., Lyu, X., Guo, H., Hu, Y.Q., 2018. Causes of ozone pollution in summer in Wuhan, Central China. Environ. Pollut. 241, 852–861. doi:10.1016/j.envpol.2018.05.042.

Zhang, L., Jacob, D.J., Boersma, K.F., Jaffe, D.A., Olson, J.R., Bowman, K.W., Worden, J.R., Thompson, A.M., Avery, M.A., Cohen, R.C., Dibb, J.E., Flocke, F.M., Fuelberg, H.E., Huey, L.G., Mcmillan, W.W., Singh, H.B., Weinheimer, A.J., 2008. Transpacific transport of ozone pollution and the effect of recent Asian emission increases on air quality in North America: an integrated analysis using satellite, aircraft, ozonesonde, and surface observations. Atmos. Chem. Phys. 8, 6117–6136. doi:10.5194/acp-8-6117-2008.

Barratt, B., Fuller, G., Analysis of the impact of Heathrow and Gatwick airport closures on local air quality during Eyjafjallajökull eruption 15th-17th April 2010 1.

Barrett, S.R.H., Britter, R.E., Waitz, I.A., 2010. Global mortality attributable to aircraft cruise emissions. Environ. Sci. Technol. 44, 7736–7742. doi:10.1021/es101325r.

Beyer, A., Wania, F., Gouin, T., Mackay, D., Matthies, M., 2003. Temperature dependence of the characteristic travel distance. Environ. Sci. Technol. 37, 766–771. doi:10.1021/es025717w.

Bolden, A.L., Kwiatkowski, C.F., Colborn, T., 2015. New look at BTEX: are ambient levels a problem? Environ. Sci. Technol. 49, 5261–5276. doi:10.1021/es505316f.

CAAC (Civil Aviation Administration of China), 2020. Civil aviation airport production statistics bulletin of 2019. http://www.caac.gov.cn/XXGK/XXGK/TJSJ/202003/t20200309_201358.html. (accessed on 15 June 2020).

Cai, C., Geng, F., Tie, X., Yu, Q., An, J., 2010. Characteristics and source apportionment of VOCs measured in Shanghai, China. Atmos. Environ. 44, 5005–5014. doi:10.1016/j.atmosenv.2010.07.059.

Carslaw, D.C., Beevers, S.D., Ropkins, K., Bell, M.C., 2006. Detecting and quantifying aircraft and other on-airport contributions to ambient nitrogen oxides in the vicinity of a large international airport. Atmos. Environ. 40, 5424–5434. doi:10.1016/j.atmosenv.2006.04.062.

Carslaw, D.C., Ropkins, K., 2012. openair — An R package for air quality data analysis. Environ. Modell. Softw. 27–28, 52–61. doi:10.1016/j.envsoft.2011.09.008.

Carslaw, D.C., Williams, M.L., Barratt, B., 2012. A short-term intervention study — Impact of airport closure due to the eruption of Eyjafjallajökull on near-field air quality. Atmos. Environ. 54, 328–336. doi:10.1016/j.atmosenv.2012.02.020.

Carslaw, D.C., 2019. The openair manual - open-source tools for analysing air pollution data. Manual for version 2.6-6. University of York.

Chen, D., Sun, J., 2018. Fuel and emission reduction assessment for civil aircraft engine fleet on-wing washing. Transp. Res. D: Transp. Environ. 65, 324–331. doi:10.1016/j.trd.2018.05.013.

Childers, J.W., Witherspoon, C.L., Smith, L.B., Pleil, J.D., 2000. Real-time and integrated measurement of potential human exposure to particle-bound polycyclic aromatic hydrocarbons (PAHs) from aircraft exhaust. Environ. Health Perspect. 108, 10.

Dumanoglu, Y., Kara, M., Altiok, H., Odabasi, M., Elbir, T., Bayram, A., 2014. Spatial and seasonal variation and source apportionment of volatile organic compounds (VOCs) in a heavily industrialized region. Atmos. Environ. 98, 168–178. doi:10.1016/j.atmosenv.2014.08.048.

Fine, P.M., 2007. Community-Scale Air Toxics Monitoringssun Valley Neighborhood and General Aviation Airport. U.S. EPA Air Toxics Data Analysis Workshop Presentation, Chicago, IL.

Grange, S.K., Lewis, A.C., Carslaw, D.C., 2016. Source apportionment advances using polar plots of bivariate correlation and regression statistics. Atmos. Environ. 145, 128–134. doi:10.1016/j.atmosenv.2016.09.016.

Hassan, M., Pfaender, H., Mavris, D., 2018. Probabilistic assessment of aviation CO_2 emission targets. Transp. Res. D: Transp. Environ. 63, 362–376. doi:10.1016/j.trd.2018.06.006.

Hertel, O., Jensen, S.S., Ketzel, M., Becker, T., Peel, R.G., Ørby, P.V., et al., 2013. Utilizing monitoring data and spatial analysis tools for exposure assessment of atmospheric pol- lutants in Denmark. In: Occurrence, Fate and Impact of Atmospheric Pollutants on Environmental and Human Health, ACS Symposium Series. American Chemical Society, pp. 95–122.

Hien, P.D., Hangartner, M., Fabian, S., Tan, P.M., 2014. Concentrations of NO_2, SO_2, and benzene across Hanoi measured by passive diffusion samplers. Atmos. Environ. 88, 66–73. doi:10.1016/j.atmosenv.2014.01.036.

Holmes, C.D., Tang, Q., Prather, M.J., 2011. Uncertainties in climate assessment for the case of aviation NO. Proc. Natl. Acad. Sci. U. S. A. 108, 10997–11002. doi:10.1073/pnas.1101458108.

Hu, S., Fruin, S., Kozawa, K., Mara, S., Winer, A.M., Paulson, S.E., 2009. Aircraft emission impacts in a neighborhood adjacent to a general aviation airport in Southern California. Environ. Sci. Technol. 43, 8039–8045. doi:10.1021/es900975f.

Hudda, N., Gould, T., Hartin, K., Larson, T.V., Fruin, S.A., 2014. Emissions from an international airport increase particle number concentrations 4-fold at 10 km downwind. Environ. Sci. Technol. 48, 6628–6635. doi:10.1021/es5001566.

Hudda, N., Simon, M.C., Zamore, W., Durant, J.L., 2018. Aviation-related impacts on ultrafine particle number concentrations outside and inside residences near an airport. Environ. Sci. Technol. 52, 1765–1772. doi:10.1021/acs.est.7b05593.

ICAO (International Civil Aviation Organization), 2019. ICAO long-term traffic forecasts passenger and cargo. https://www.icao.int/sustainability/Documents/LTF_Charts-Results_2018edition.pdf. (accessed on 20 May 2020).

IEA (International Energy Agency), 2020. Global Energy Review 2020.

Jones, A.M., Harrison, R.M., Baker, J., 2010. The wind speed dependence of the concentrations of airborne particulate matter and NOx. Atmos. Environ. 44, 1682–1690. doi:10.1016/j.atmosenv.2010.01.007.

Jung, K.-H., Artigas, F., Shin, J.Y., 2011. Personal, indoor, and outdoor exposure to VOCs in the immediate vicinity of a local airport. Environ. Monit. Assess. 173, 555–567. doi:10.1007/s10661-010-1404-9.

Kesgin, U., 2006. Aircraft emissions at Turkish airports. Energy 31, 372–384. doi:10.1016/j.energy.2005.01.012.

Le, T., Wang, Y., Liu, L., Yang, J., Yung, Y.L., Li, G., Seinfeld, J.H., 2020. Unexpected air pollution with marked emission reductions during the COVID-19 outbreak in China. Science 369, 702–706. doi:10.1126/science.abb7431.

Lee, D.S., Fahey, D.W., Forster, P.M., Newton, P.J., Wit, R.C.N., Lim, L.L., et al., 2009. Aviation and global climate change in the 21st century. Atmos. Environ. 43, 3520–3537. doi:10.1016/j.atmosenv.2009.04.024.

Lee, D.S., Pitari, G., Grewe, V., Gierens, K., Penner, J.E., Petzold, A., Prather, M.J., Schumann, U., Bais, A., Berntsen, T., 2010. Transport impacts on atmosphere and climate: aviation. Atmos. Environ. 44, 4678–4734. doi:10.1016/j.atmosenv.2009.06.005.

Lee, D.S., Fahey, D.W., Skowron, A., Allen, M.R., Burkhardt, U., Chen, Q., et al., 2021. The contribution of global aviation to anthropogenic climate forcing for 2000 to 2018. Atmos. Environ. 244, 117834. doi:10.1016/j.atmosenv.2020.117834.

Lee, H., Olsen, S.C., Wuebbles, D.J., Youn, D., 2013. Impacts of aircraft emissions on the air quality near the ground. Atmos. Chem. Phys. 13, 5505–5522. doi:10.5194/acp-13-5505-2013.

Levy, J.I., Woody, M., Baek, B.H., Shankar, U., Arunachalam, S., 2012. Current and future particulate-matter-related mortality risks in the United States from aviation emissions during landing and takeoff: mortality risks from aviation emissions during landing and takeoff. Risk Anal. 32, 237–249. doi:10.1111/j.1539-6924.2011.01660.x.

Levy, M., Zhang, R., Zheng, J., Zhang, A.L., Xu, W., Gomez-Hernandez, M., et al., 2014. Measurements of nitrous acid (HONO) using ion drift-chemical ionization mass spectrometry during the 2009 SHARP field campaign. Atmos. Environ. 94, 231–240. doi:10.1016/j.atmosenv.2014.05.024.

Liu, Z., Wang, Y., Gu, D., Zhao, C., Huey, L.G., Stickel, R., et al., 2012. Summertime photochemistry during CAREBeijing-2007: RO_x budgets and O_3 formation. Atmos. Chem. Phys. 12, 7737–7752. doi:10.5194/acp-12-7737-2012.

Lu, K., Zhang, Y., Su, H., Brauers, T., Chou, C.C., Hofzumahaus, A., et al., 2010. Oxidant (O_3 + NO_2) production processes and formation regimes in Beijing. J. Geophys. Res. 115, D07303. doi:10.1029/2009JD012714.

Mao, L., Liu, R., Liao, W., Wang, X., Shao, M., Liu, S.C., et al., 2019. An observation-based perspective of winter haze days in four major polluted regions of China. Nat. Sci. Rev. 6, 515–523. doi:10.1093/nsr/nwy118.

Masiol, M., Harrison, R.M., 2015. Quantification of air quality impacts of London Heathrow Airport (UK) from 2005 to 2012. Atmos. Environ. 116, 308–319. doi:10.1016/j.atmosenv.2015.06.048.

MEE (Ministry of Ecology and Environment of China), 2018a. Technical specifications for operation and quality control of ambient air quality automated monitoring system for particulate matter (PM10 and PM2.5). https://www.mee.gov.cn/ywgz/fgbz/bz/bzwb/jcffbz/201808/W020180815358016693515.pdf. (accessed on 31 May 2020).

MEE (Ministry of Ecology and Environment of China), 2018b. Technical specifications for operation and quality control of ambient air quality continuous automated monitoring system for SO2, NO2, O3 and CO. https://www.mee.gov.cn/ywgz/fgbz/bz/bzwb/jcffbz/201808/W020180815358674459089.pdf. (accessed on 31 May 2020).

Molina, L.T., de Foy, B., Vázquez Martińez, O., Páramo Figuero, V.H., 2009. Air quality, weather and climate in Mexico City. WMO Bull. 58 (January 2009).

Morris, G.A., Rosenfield, J.E., Schoeberl, M.R., Jackman, C.H., 2003. Potential impact of subsonic and supersonic aircraft exhaust on water vapor in the lower stratosphere assessed via a trajectory model. J. Geophys. Res.: Atmos. 108. doi:10.1029/2002JD002614.

Murphy, J.G., Day, D.A., Cleary, P.A., Wooldridge, P.J., Millet, D.B., Goldstein, A.H., et al., 2007. The weekend effect within and downwind of Sacramento – part 1: observations of ozone, nitrogen oxides, and VOC reactivity. Atmos. Chem. Phys. 7, 5327–5339. doi:10.5194/acp-7-5327-2007.

Olsen, S.C., Wuebbles, D.J., Owen, B., 2013. Comparison of global 3-D aviation emissions datasets. Atmos. Chem. Phys. 13, 429–441. doi:10.5194/acp-13-429-2013.

R Core Team, 2019. R: A language and environment for statistical computing. R Foundation for Statistical Computing, Vienna, Austria.

Ran, L., Zhao, C., Geng, F., Tie, X., Tang, X., Peng, L., et al., 2009. Ozone photochemical production in urban Shanghai, China: Analysis based on ground level observations. J. Geophys. Res. 114. doi:10.1029/2008JD010752.

Schürmann, G., Schäfer, K., Jahn, C., Hoffmann, H., Bauerfeind, M., Fleuti, E., et al., 2007. The impact of NOx, CO and VOC emissions on the air quality of Zurich airport. Atmos. Environ. 41, 103–118. doi:10.1016/j.atmosenv.2006.07.030.

Shiraiwa, M., Ueda, K., Pozzer, A., Lammel, G., Kampf, C.J., Fushimi, A., et al., 2017. Aerosol health effects from molecular to global scales. Environ. Sci. Technol. 51, 13545–13567. doi:10.1021/acs.est.7b04417.

Sicard, P., De Marco, A., Agathokleous, E., Feng, Z., Xu, X., Paoletti, E., et al., 2020. Amplified ozone pollution in cities during the COVID-19 lockdown. Sci. Total Environ. 735, 139542. doi:10.1016/j.scitotenv.2020.139542.

Sillman, S., 1995. The use of NOy, H_2O_2, and HNO_3 as indicators for ozone-NOx- hydrocarbon sensitivity in urban locations. J. Geophys. Res. 100, 14175–14188.

Sillman, S., 1999. The relation between ozone, NOx and hydrocarbons in urban and polluted rural environments. Atmos. Environ. 33, 1821–1845. doi:10.1016/S1352-2310(98)00345-8.

Solberg, S., Bergström, R., Langner, J., Laurila, T., Lindskog, A., 2005. Changes in Nordic surface ozone episodes due to European emission reductions in the 1990s. Atmos. Environ. 39, 179–192. doi:10.1016/j.atmosenv.2004.08.049.

Song, S.-K., Shon, Z.-H., Kang, Y.-H., 2015. Comparison of impacts of aircraft emissions within the boundary layer on the regional ozone in South Korea. Atmos. Environ. 117, 169–179. doi:10.1016/j.atmosenv.2015.07.010.

Stettler, M.E.J., Eastham, S., Barrett, S.R.H., 2011. Air quality and public health impacts of UK airports. Part I: Emissions. Atmos. Environ. 45, 5415–5424. doi:10.1016/j.atmosenv.2011.07.012.

Stoll, C., Mehling, M.A., 2020. COVID-19: clinching the climate opportunity. One Earth 3, 400–404. doi:10.1016/j.oneear.2020.09.003.

Tan, Z., Lu, K., Jiang, M., Su, R., Wang, H., Lou, S., et al., 2019. Daytime atmospheric oxidation capacity in four Chinese megacities during the photochemically polluted season: a case study based on box model simulation. Atmos. Chem. Phys. 19, 3493–3513. doi:10.5194/acp-19-3493-2019.

Tomlin, A.S., Smalley, R.J., Tate, J.E., Barlow, J.F., Belcher, S.E., Arnold, S.J., et al., 2009. A field study of factors influencing the concentrations of a traffic-related pollutant in the vicinity of a complex urban junction. Atmos. Environ. 43, 5027–5037. doi:10.1016/j.atmosenv.2009.06.047.

Unal, A., Hu, Y., Chang, M.E., Talat Odman, M., Russell, A.G., 2005. Airport related emissions and impacts on air quality: application to the Atlanta International Airport. Atmos. Environ. 39, 5787–5798. doi:10.1016/j.atmosenv.2005.05.051.

Vaughan, A., 2020. The climate fight after coronavirus. New Scientist 247, 36–39. doi:10.1016/S0262-4079(20)31176-3.

Wang, Pengfei, Chen, K., Zhu, S., Wang, Peng, Zhang, H., 2020. Severe air pollution events not avoided by reduced anthropogenic activities during COVID-19 outbreak. Resour. Conserv. Recy. 158, 104814. doi:10.1016/j.resconrec.2020.104814.

Wang, T., Xue, L., Brimblecombe, P., Lam, Y.F., Li, L., Zhang, L., 2017. Ozone pollution in China: a review of concentrations, meteorological influences, chemical precursors, and effects. Sci. Total Environ. 575, 1582–1596. doi:10.1016/j.scitotenv.2016.10.081.

WHO (World Health Organization), 2020. Virtual press conference on COVID-19 –11 March 2020. https://www.who.int/docs/default-source/coronaviruse/transcripts/who-audio-emergencies-coronavirus-press-conference-full-and-final-11mar2020.pdf?sfvrsn=cb432bb3_2. (accessed on 15 June 2020).

Wolff, G.T., Kahlbaum, D.F., Heuss, J.M., 2013. The vanishing ozone weekday/weekend effect. J. Air Waste Manage. Assoc. 63, 292–299. doi:10.1080/10962247.2012.749312.

Woody, M., Haeng Baek, B., Adelman, Z., Omary, M., Fat Lam, Y., Jason West, J., et al., 2011. An assessment of Aviation's contribution to current and future fine particulate matter in the United States. Atmos. Environ. 45, 3424–3433. doi:10.1016/j.atmosenv.2011.03.041.

Xing, C., Liu, C., Wang, S., Chan, K.L., Gao, Y., Huang, X., et al., 2017. Observations of the vertical distributions of summertime atmospheric pollutants and the corresponding ozone production in Shanghai, China. Atmos. Chem. Phys. 17, 14275–14289. doi:10.5194/acp-17-14275-2017.

Xinhua Net, 2020. China suspends road, waterway passenger traffic into Wuhan in epidemic control. http://www.xinhuanet.com/english/2020-01/23/c_138729558.htm. (accessed on 31 May 2020).

Xu, H., Fu, Q., Yu, Y., Liu, Q., Pan, J., Cheng, J., Wang, Z., Liu, L., 2020a. Quantifying aircraft emissions of Shanghai Pudong International Airport with aircraft ground operational data. Environ. Pollut. 261, 114115. doi:10.1016/j.envpol.2020.114115.

Xu, H., Xiao, K., Cheng, J., Yu, Y., Liu, Q., Pan, J., Chen, J., Chen, F., Fu, Q., 2020b. Characterizing aircraft engine fuel and emission parameters of taxi phase for Shanghai Hongqiao International Airport with aircraft operational data. Sci. Total Environ. 720, 137431. doi:10.1016/j.scitotenv.2020.137431.

Yang, X., Cheng, S., Wang, G., Xu, R., Wang, X., Zhang, H., et al., 2018. Characterization of volatile organic compounds and the impacts on the regional ozone at an international airport. Environ. Pollut. 238, 491–499. doi:10.1016/j.envpol.2018.03.073.

Yim, S.H.L., Lee, G.L., Lee, I.H., Allroggen, F., Ashok, A., Caiazzo, F., et al., 2015. Global, regional and local health impacts of civil aviation emissions. Environ. Res. Lett. 10, 034001. doi:10.1088/1748-9326/10/3/034001.